Journal of Chemistry and Technologies

LUMINESCENT PROPERTIES OF Mn⁴⁺-DOPED α-Al₂O₃ OBTAINED BY COMBUSTION METHOD

Olena V. Khomenko*[1], Irina V. Berezovskaya[1], Nikolay I. Poletaev[2], Maria E. Khlebnikova[2], Ninel P. Efryushina[1], Vladimir P. Dotsenko*[1]

[1] *A. V. Bogatsky Physico-Chemical Institute, National Academy of Sciences of Ukraine, 86 Lustdorfskaya doroga, Odessa, 65080 Ukraine*

[2] *Institute of Combustion and Advanced Technologies, I. I. Mechnikov Odessa National University, 2, Dvoryanskaya, Odessa, 65082 Ukraine*

Abstract

The Mn^{4+}-doped α-Al_2O_3 with particle size of 70–600 nm was obtained by combustion method. Based on the results of luminescence measurements, the crystal-field strength (Dq) and Racah parameters (B, C) for Mn^{4+} in α-Al_2O_3 were determined using a pure electronic transition approach. The obtained values of Dq (1898 cm⁻¹) and nephelauxetic parameter β_1 (0.95) for Mn^{4+} ions in α-Al_2O_3 are consistent with those of Mn^{4+} in other oxide compounds. In particular, the Dq/B value of 2.77 indicates a strong crystal field environment of the Mn^{4+} ions in the α-Al_2O_3 lattice. A comparison with literature data for Cr^{3+} in α-Al_2O_3 was also carried out. The composites of general formula α-Al_2O_3 : Mn^{4+}, Mg^{2+}/$Gd_3Al_5O_{12}$:Ce^{3+} had been also obtained. It is shown that these materials demonstrate the intense broadband emission with maxima at about 585 and 678 nm. The broad band with a maximum at 585 nm is caused by the 5d→4f transitions of Ce^{3+} ions in $Gd_3Al_5O_{12}$, whereas the band at 678 nm is caused by the Mn^{4+} ^2E_g→$^4A_{2g}$ transitions in α-Al_2O_3. The emission color changes from yellow to deep red with increasing content of α-Al_2O_3:Mn^{4+}, Mg^{2+}, and the luminescence quantum efficiency of the composites was found as high as 0.60.

Keywords: aluminum oxide; combustion synthesis; Mn^{4+}; luminescence; Racah parameters; luminescence composites.

ЛЮМІНЕСЦЕНТНІ ВЛАСТИВОСТІ α-Al₂O₃ : Mn⁴⁺, ОДЕРЖАНОГО МЕТОДОМ ГОРІННЯ

Олена В. Хоменко*[1], Ірина В. Березовська[1], Микола І. Полєтаєв[2], Марія Є. Хлєбнікова[2], Нінель П. Єфрюшина[1], Володимир П. Доценко*[1]

[1] *Фізико-хімічний інститут ім. О. В. Богатського НАН України, Люстдорфська дорога, 86, Одеса, 65080, Україна*

[2] *Інститут горіння та нетрадиційних технологій, Одеський національний університет ім. І. І. Мечнікова, вул. Дворянська, 2, Одеса, 65082, Україна*

Анотація

Методом горіння одержано легований Mn^{4+} α-Al_2O_3 з розміром частинок 70–600 нм. На підставі результатів люмінесцентних вимірювань в рамках наближення чисто електронних переходів розраховано силу кристалічного поля (Dq) та параметри Рака (B, C) для Mn^{4+} в α-Al_2O_3. Одержані значення Dq (1898 см⁻¹) та нефелауксетичного параметра β_1 (0.95) для іонів Mn^{4+} в α-Al_2O_3 узгоджуються зі значеннями цих параметрів для Mn^{4+} в інших оксидних сполуках. Зокрема, величина Dq/B = 2.77 вказує, що іони Mn^{4+} займають в гратці α-Al_2O_3 октаедричні позиції Al з великою силою кристалічного поля. Проведено порівняння з літературними даними для іонів Cr^{3+} в α-Al_2O_3. Одержано композити загальної формули α-Al_2O_3:Mn^{4+}, Mg^{2+}/$Gd_3Al_5O_{12}$: Ce^{3+}. Показано, що ці матеріали демонструють інтенсивне широкосмугове випромінювання з максимумами при ~585 і 678 нм. Широка смуга з максимумом при 585 нм зумовлена переходами 5d→4f іонів Ce^{3+} в $Gd_3Al_5O_{12}$, тоді як смуга при 678 нм зумовлена переходами ^2E_g→$^4A_{2g}$ Mn^{4+} в α-Al_2O_3. Колір випромінювання змінюється від жовтого до насичено-червоного із збільшенням вмісту α-Al_2O_3:Mn^{4+}, Mg^{2+}, а квантова ефективність люмінесценції композитів досягає 0.60.

Ключові слова: оксид алюмінію; синтез методом горіння; Mn^{4+}; люмінесценція; параметри Рака; люмінесцентні композити.

Introduction

In recent years, crystals doped with tetravalent manganese ions (Mn^{4+}) have been adopted in various fields, such as general lighting [1; 2], plant cultivation light-emitting diodes (LED) [3] and LED displays [4]. The luminescence properties of Mn^{4+} in inorganic materials have been examined in a number of papers [2; 5–7]. It is known that due to a high effective positive charge, Mn^{4+} tends to occupy octahedral sites with large crystal-field strength, and only transitions from the ^2E_g state to the $^4A_{2g}$ ground state are observed in the emission spectra. The $^2E_g \rightarrow {}^4A_{2g}$ electronic transitions are spin-forbidden, but they become partially allowed due to mixing of the ^2E_g and $^4T_{2g}$ states by spin-orbit interaction. Typically, the emission spectra of Mn^{4+} consist of narrow zero-phonon lines (ZPL or R-lines) and corresponding vibronic sidebands. It is shown that the energy position of the ^2E_g state is nearly independent on the crystal-field strength, but it is substantially dependent on the covalency of the Mn^{4+}-ligand bond. The influence of the main lattice on the luminescence properties of transition metal ions with the $3d^3$-configuration (Cr^{3+}, Mn^{4+}) is usually described by a number of parameters, such as the crystal-field strength *(Dq)* and the Racah parameters (*B*, *C*) in conjunction with the Tanabe-Sugano diagram [2; 6; 7]. The crystal-field strength describes an interaction of the d-electrons with the electrostatic field of the ligands, while the Racah parameters characterize the effects of inter-electronic repulsion.

Because of the covalent interaction between Mn^{4+} and anions (or ligands), the Racah parameters are reduced in comparison with the free ion values (B_0= 1160 cm^{-1}, C_0= 4303 cm^{-1}), and this effect can be expressed by the so called nephelauxetic parameter β_1 [5; 6]:

$$\beta_1 = \sqrt{\left(\frac{B}{B_0}\right)^2 + \left(\frac{C}{C_0}\right)^2} \qquad (1)$$

In 2015 it has been reported that energy of the Mn^{4+} ^2E_g state ($E(^2E_g)$) is a linear function of the parameter β_1 for different kinds of host materials, including fluorides, silicates and also numerous aluminates [5; 6]. In this regard, it seems rather surprising that one of few exceptions from this trend is thermodynamically stable polymorph (α) of Al_2O_3 [5; 6]. The reasons for this have not been clarified. It should be noted that in α-Al_2O_3, each Al^{3+} is surrounded by a trigonally distorted octahedron of six oxygen atoms.

Very recently the authors [8] have reported the optical properties of red emitting ceramics of composition α-Al_2O_3:Mn^{4+}, Mg^{2+}. Based on the results obtained, the calculated ratio of *Dq* to *B* for the Mn^{4+} appeared as 1.74. This value of *Dq/B* implies a weak crystal field surrounding of the Mn^{4+} ions in α-Al_2O_3 host [8]. This conclusion seems to be doubtful, since, as it was mentioned above, the Mn^{4+} ions are always experiencing the strong crystal field, i.e. the *Dq/B* value should be ≥ 2.2 [2; 6; 7].

It should be also noted that α-Al_2O_3 doped with Mn^{4+} appears as a promising phosphor for non-contact luminescence thermometry [9]. In view of the importance of Mn^{4+}-doped α-Al_2O_3 as a functional material and also as a model system to analyse different aspects of spectroscopy of the $3d^3$ ions (Mn^{4+}, Cr^{3+}, V^{2+}) in inorganic compounds, the aim of this study was finding out the reasons for deviation of the data for Mn^{4+}-doped α-Al_2O_3 from linear dependence of energy of the ^2E_g state on β_1 [5; 6]. Besides, the present work was motivated by an interest to obtain luminescent composites based on Al_2O_3:Mn^{4+} and, in particular, ones of general formula Al_2O_3:Mn^{4+}/$Gd_3Al_5O_{12}$: Ce^{3+}. Gadolinium aluminum garnet $Gd_3Al_5O_{12}$ (GdAG) doped with Ce^{3+} ions is known as an effective phosphor for medium power white LEDs [10; 11]. Also, the development of nanocomposites based on GdAG : Ce^{3+} has been recently reported for imaging and photodynamic therapy of cancer cells [12].

Experimental

A powder sample of Mn-doped Al_2O_3 with particles sizes of 10–70 nm was prepared by a gas-dispersed synthesis (GDS). This method is based on the combustion of powdered metals due to exothermic oxidizing reactions between them and a gaseous oxidizer (typically O_2) [13], and it is shown to provide favorable morphology of Al_2O_3 particles and good dispersibility of the final product in various media [13–15]. The details of experimental apparatus used for the GDS of nanosized Mn-doped Al_2O_3 were described previously [13]. As it was also found earlier [16], the resulting powders consist of a mixture of transition aluminas (δ^*,δ and θ-polymorphs), and a part of Mn ions exists in the oxidation state +2 and occupies tetrahedral positions in δ^*-Al_2O_3, causing a broadband luminescence with a maximum at ~520 nm. It is shown that additional annealing in air at temperatures ≥1130°C results in the formation of stable α-polymorph. The δ^*,θ→α-Al_2O_3 phase transition is followed by oxidation of Mn^{2+}/Mn^{3+} ions and the formation of some amount of manganese ions in the oxidation

state +4 on octahedral Al positions [16]. In Al_2O_3, the stabilization of Mn^{4+} can be provided through the formation of cation (Al) vacancies [17; 18] or by the introduction into the host lattice of charge-compensating ions, such as Mg^{2+} [8; 19].

To obtain Mn-doped α-Al_2O_3 with a nominal Mn concentration of 0.1 at.%, the appropriate amount of $MnCl_2$ (99.99 %) was dissolved in ethanol. Then, the solution was gradually added, while thoroughly mixing, to calculated amounts of Al powder (purity 99.7 %) with an average size of 4.8 μm. After drying in air, the as-obtained mixture was dispersed in nitrogen and injected through an inner tube into oxygen stream. After ignition by an external source a stable two-phase diffusion dust flame was observed. The condensed products of aluminum combustion had been collected using a polyethylene terephthalate filter. Some part of the sample obtained was then used to prepare double doped α-Al_2O_3:Mn^{4+}, Mg^{2+} and luminescence composites α-Al_2O_3 : Mn^{4+}, Mg^{2+}/GdAG : Ce^{3+}. For this purpose the calculated amount of magnesium chloride ($MgCl_2·6H_2O$) was dissolved in ethanol and added to the nanosized Mn-doped Al_2O_3 to improve the luminescence efficiency of final products. This reagent was used in the amount corresponding to the atomic Mg/Mn ratio of 1. After drying at 110 °C all the samples were annealed in air at the temperature of 1300°C during 6 hpurs.

Luminescence composites α-Al_2O_3:Mn^{4+}, Mg^{2+}/GdAG : Ce^{3+}, with different weight ratios of the components, had been obtained by thoroughly mixing of α-Al_2O_3 : Mn^{4+}, Mg^{2+} and GdAG : Ce^{3+} powders in ethanol, followed by drying and annealing in air at the temperature of 1300 °C during for 2 hours. Ce^{3+}-doped gadolinium aluminum garnet GdAG : Ce^{3+} with a nominal Ce^{3+} concentration of 1 at.% was previously synthesized by the co-precipitation of rare earth metals and aluminum hydroxides and their further thermal decomposition [11]. X-ray diffraction (XRD) studies had been carried out on a Rigaku Ultima IV diffractometer using Cu Ka radiation (λ = 1.5418 Å). Transmission electron microscopy (TEM) images of the samples had been obtained on a Philips EM-400 transmission electron microscope. The emission and excitation spectra in UV-visible region were recorded at 293 and 77 K using a Fluorolog FL-3-22 (Horiba Jobin Yvon) spectrofluorometer equipped with a xenon lamp. Diffuse reflection spectra had been obtained on a Perkin-Elmer Lambda 9 spectrometer.

Results and discussion

Fig. 1 shows the XRD patterns of Mn-doped α-Al_2O_3 and α-Al_2O_3 : Mn^{4+}, Mg^{2+}. One can see that the XRD patterns of the samples annealed at 1300 °C for 6 h match well with data from JCPDS database for pure α-Al_2O_3 (JCPDS Card 10-173), but trace amounts of θ-Al_2O_3 are also detected. It should be noted that the introduction of Mn and Mg is not accompanied by any changes in the XRD patterns. It is an expected result because of the relatively small concentrations of Mn and Mg in the samples. TEM image of as-prepared α-Al_2O_3 : Mn is presented in Fig. 2.
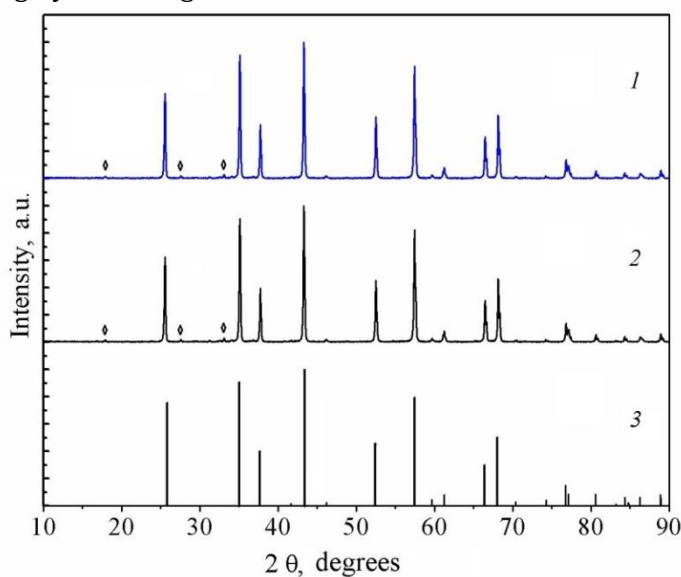
Fig. 1. Comparison of X-ray diffraction patterns of as-prepared Mn-doped α-Al_2O_3 (1) and α-Al_2O_3:Mn^{4+},Mg^{2+} (*2*) with data from JCPDS database (JCPDS Card 10-173) for pure α-Al_2O_3 (3). Reflections associated with the presence of trace amounts (≤2%) of θ-Al_2O_3 are shown by symbols (◊)

As it can be seen, the sample consists of submicron-size (200–600 nm) aggregates of vermicular shape, although some amount of nanosized particles is also present as individual crystallites. It should be noted that electron microscopy data obtained in the present study did not also reveal any significant effect of Mn (Mg) on the particle size distribution of the final products. The Kubelka-Munk transformed diffuse reflection spectrum of as-prepared α-Al$_2$O$_3$: Mn appeared to be similar to those reported for Mn^{3+}-doped α-Al$_2$O$_3$ [20]. It consists of wide overlapping bands in the 400–620 nm area. There are two local maxima at ~490 and 537 nm. Analogous absorption spectra had been also obtained for Mn^{3+}-doped

yttrium aluminates Y$_3$Al$_5$O$_{12}$ [21] and YAlO$_3$ [22], and they had been interpreted as a result of $^5E_g \rightarrow {}^5T_2$ transitions in Mn^{3+} ions at the aluminum octahedral (Al$_{oct}$) po-sitions. The substantial half-width (~4000 cm^{-1}) of Mn^{3+} absorption band in Y$_3$Al$_5$O$_{12}$ was attributed to Jahn-Teller splitting of both ^5E_g, $^5T_2$ states of Mn^{3+} [21]. Thus, the broad absorption bands in the diffuse reflection spectrum of as-prepared α-Al$_2$O$_3$: Mn are mainly caused by the $^5E_g \rightarrow {}^5T_2$ transitions of Mn^{3+} ions occupying the Al$_{oct}$ positions.

The emission and luminescence excitation spectra of the α-Al$_2$O$_3$: Mn at 293 and 77 K are compared in Figs. 3 and 4.
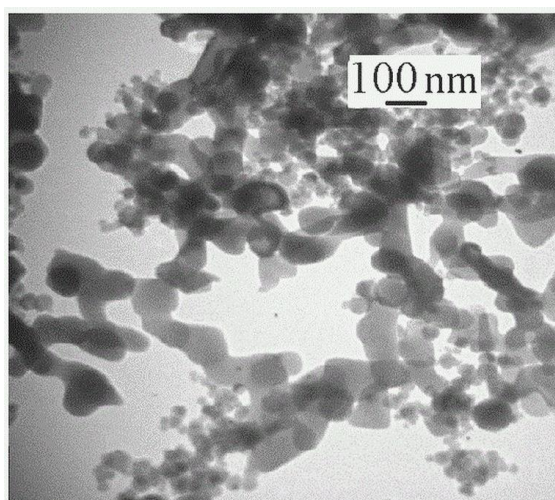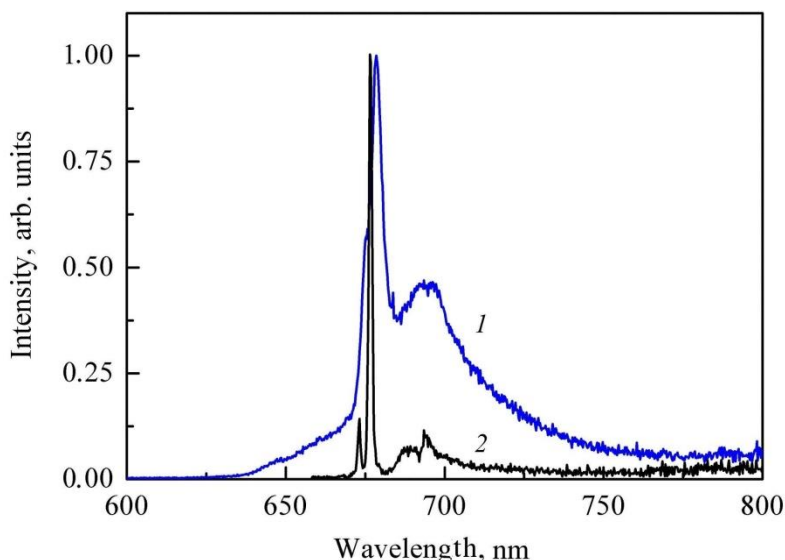

Fig. 2. TEM image of as-prepared α-Al$_2$O$_3$:Mn

Fig. 3. Comparison of the normalized emission spectra of Mn^{4+} in as-prepared α-Al$_2$O$_3$:Mn$^{3+/4+}$ upon excitation with λ_{exc}= 460 nm at 293 K (*1*) and 77 K (*2*)
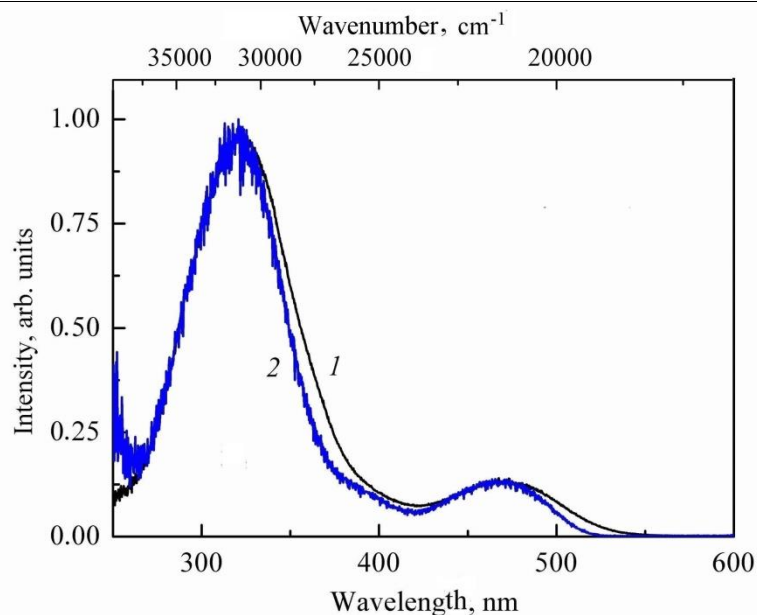
Fig. 4. Comparison of the excitation spectra for the Mn⁴⁺ emission (λₑₘ= 678 nm) in as-prepared α-Al₂O₃:Mn³⁺/⁴⁺ recorded at 293 K (*1*) and 77 K (*2*)

At the room temperature the emission spectrum contains an intense band at 678 nm with a long-wavelength tail extending up to 770 nm. There is no doubt about its nature, because the identical spectrum was reported earlier for Mn⁴⁺-doped α-Al₂O₃ [19; 20], and it was interpreted as a result of the $^2E_g \to {}^4A_{2g}$ transition and vibronic transitions, respectively. A deviation from perfect octahedral symmetry and spin-orbit interaction are known to split the ^2E_g state into two components, and they result in so-called $R_{1,2}$-lines luminescence, which is caused with the parity- and spin-forbidden $^2E_g \to {}^4A_{2g}$ transitions of Mn⁴⁺ ions. It is seen from Fig. 3 that at 77 K the emission spectrum consists of two relatively narrow lines at 676.4 nm (14784 cm⁻¹) and 672.9 nm (14861 cm⁻¹), known as R_1 and R_2-lines, and vibronic sideband at 683–710 nm.

It should be noted that in the 77–293 K range the sample did not show any emission that could be attributed to either Mn³⁺ or Mn²⁺ ions. This agrees with the conclusion of the authors [20] about the absence of any luminescence from Mn³⁺ ions in α-Al₂O₃ even at 4.2 K, which was explained by a strong Jahn-Teller effect.

It can be seen from Fig. 4 that at 293 K the excitation spectrum for the luminescence of Mn⁴⁺ ions in α-Al₂O₃ consists of a broad intense band with a maximum at 323 nm (30960 cm⁻¹) and a less intense one at 476 nm (21008 cm⁻¹). The latter is obviously connected with the $^4A_{2g} \to {}^4T_{2g}$ transition of Mn⁴⁺ ions, while the assignment of the former band is not unambiguous. In Ref. [8] the broad band at about 316 nm was attributed to the $^4A_{2g} \to {}^4T_{1g}$ transition of Mn⁴⁺ ions, whereas the

authors [20] assigned this feature to a charge-transfer transition from 2p orbitals of O²⁻ to the Mn⁴⁺ vacant orbitals. An analogous band at 317 nm was shown to be present in the luminescence excitation spectra for Mn⁴⁺ ions in GdAlO₃. Based on the calculations for Mn⁴⁺ energy levels in GdAlO₃ in limits of the exchange charge model of crystal-field theory, it was interpreted as a superposition of the O²⁻→Mn⁴⁺ charge transfer band and a band caused by the $^4A_{2g} \to {}^4T_{1g}$ transition of Mn⁴⁺ ions located in Al_oct positions [23]. The excitation spectrum of the Mn⁴⁺ luminescence in as-prepared α-Al₂O₃:Mn³⁺/⁴⁺ recorded at 77 K is similar to that at the room temperature. But in addition to the bands at 323 and 476 nm, an arm in the 380–420 nm range is distinctly observed, suggesting a superposition character of the 323 nm band.

Usually, instead of zero-phonon line (ZPL) energies, the energies relating to the maxima of $^4A_{2g} \to {}^4T_{1g}, {}^4T_{2g}$ excitation bands of Mn⁴⁺ are used to determine the values of *Dq, B* and *C*. However, this often leads to a big error or uncertainty in the estimation of the Racah parameters. In our opinion, this is also the main reason for the unreliable *Dq/B* value of 1.74 obtained in Ref. [8] for Mn⁴⁺ in α-Al₂O₃, and the essential deviation of the data for Mn⁴-doped α-Al₂O₃ from the linear dependence of $E(^2E_g)$ on β_1 [5; 6]. Meanwhile, even for the ordered crystals, an accurate determination of the ZPL energies of the $^4A_{2g} \to {}^4T_{1g}, {}^4T_{2g}$ transitions is very difficult because of the crystal-field splitting of $^4T_{1g}, {}^4T_{2g}$ levels, and an interaction of Mn⁴⁺ with lattice vibration modes. To overcome this problem a new approach based

on the ligand field theory had been proposed recently [7; 24]. In this approach the following expressions are applied to calculate the Racah and crystal-field related parameters:

$$E\left(^4T_{2g}\right) = 10\, Dq \quad (2);$$

$$B = 6.18Dq - \frac{1}{2}[(12.36Dq)^2 - 2.22E(^2E_g)\, Dq]^{1/2} \quad (3);$$

$$\frac{C}{B} = 4.7 \quad (4);$$

$$E\left(^4T_{1g}\right)_{ZPL} = 7.5\mathrm{B} + 15Dq - \frac{Dq}{2}\left[\left(\frac{15B}{Dq}+10\right)^2 - \frac{480B}{Dq}\right]^{\frac{1}{2}} \quad (5);$$

Since in the case of α-Al$_2$O$_3$:Mn^{4+} the fine structure of interest here turns out to be obscured, the wavelength where the excitation intensity has dropped to ~3% on the long wavelength side of the $^4A_{2g} \rightarrow {}^4T_{2g}$ excitation band was used in the present study as a rough estimate for $E(^4T_{2g})_{ZPL}$ of the Mn^{4+} ions in the α-Al$_2$O$_3$. Obviously, the ZPL of the $^4A_{2g} \rightarrow {}^4T_{2g}$ excitation band should be located near its long-wavelength tail, and the used assumption conforms to the results of calculations based on the Franck-Condon analysis model for numerous Mn^{4+}-doped inorganic compounds [2; 7; 24]. From the positions of the R$_1$-line (14784 cm^{-1}) and $^4A_{2g} \rightarrow {}^4T_{2g}$ excitation band in the spectra at 77 K (Figs. 3 and 4), the Racah and crystal-field related parameters for Mn^{4+} were calculated using Eqs. (2)–(5). The obtained data are presented in the Table and compared with those for Cr^{3+} ions in α-Al$_2$O$_3$ [25; 26].

Table

Comparison of the crystal-field strength *Dq*, Racah parameters and nephelauxetic parameter β_1 for Mn^{4+} and Cr^{3+} ions in α-Al$_2$O$_3$ (T= 77 K)

Ion	$E(^2E_g)$ (см$^{-1}$)	Dq (см$^{-1}$)	B (см$^{-1}$)	C (см$^{-1}$)	Dq/B	β_1	Ref.
Cr^{3+}	14424	1676	669	3144	2.50	1.09	[25,26]
Mn^{4+}	14784	1898	684	3215	2.77	0.95	This work

As it can be seen from the Table, the crystal-field strength for Mn^{4+} in the α-Al$_2$O$_3$ is 1898 cm^{-1}, which exceeds that for Cr^{3+} (*Dq*= 1676 cm^{-1}). This is the expected result because of the bigger formal charge and the smaller ionic radius of Mn^{4+} compared to Cr^{3+}. Since the electronegativity of Mn^{4+} (χ= 1.912) is higher than that of Cr^{3+} (χ = 1.587) [27], it can be expected that the covalency of the Mn^{4+}-O bond should be bigger than that of the Cr^{3+}-O bond. This is also conformed to the obtained data: the β_1 value of 0.95 for Mn^{4+} in the α-Al$_2$O$_3$ is found to be smaller than that (β_1= 1.09) reported previously for Cr^{3+} ions in this compound [9; 25]. The reliability of the results obtained for the Mn^{4+}-doped α-Al$_2$O$_3$ is confirmed by the fact that the calculated excited state energies divided by *B* and plotted against *Dq/B*, fall on the Tanabe-Sugano diagram well. In this context, it is worth noting that the *Dq/B* value of 2.77 (see the Table) indicates a strong crystal field surrounding of the Mn^{4+} ions in the α-Al$_2$O$_3$ lattice.

Fig. 5 shows the dependence of energy of the Mn^{4+} ^2E_g state on the nephelauxetic parameter β_1 for a large group of oxide compounds. With the exception of α-Al$_2$O$_3$, the $E(^2E_g)$ and β_1 values for these compounds were taken from Ref. [2] and the solid line represents the least-squares fit of the data by the expression proposed also in [2]:

$$E\left(^2E_g\right) = 7.63 \times 10^3 \beta_1 + 7.52 \times 10^3 \text{ (in cm}^{-1}\text{ units)} \quad (6).$$

It is seen that the data for the Mn^{4+}-doped α-Al$_2$O$_3$ are in very good agreement with the dependence described by Eq. 6. Thus, the values of Racah and crystal-field related parameters for Mn^{4+} ions in α-Al$_2$O$_3$ obtained using the ZPL approach, conform to those of Mn^{4+} in other oxide compounds and also to those of Cr^{3+} in this host lattice.
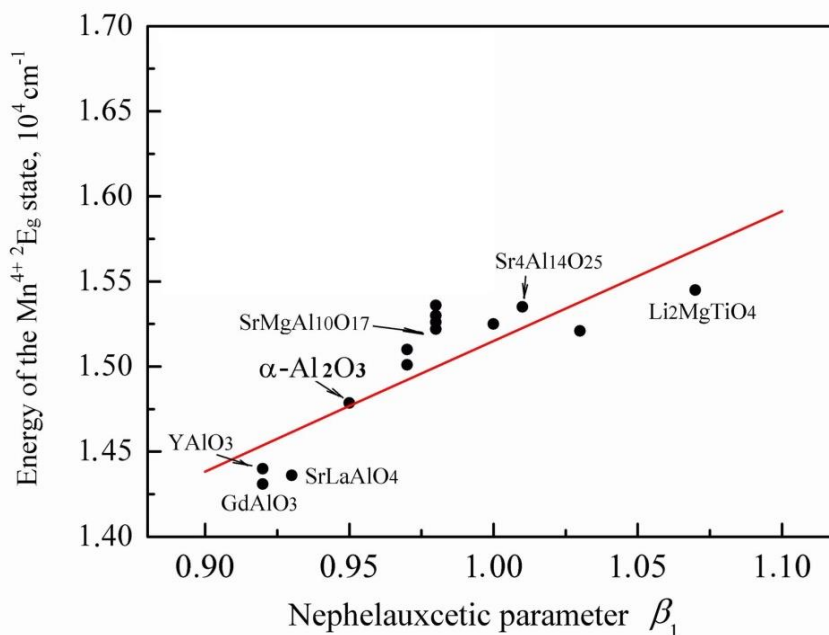
Fig. 5. Dependence of energy of the Mn^{4+} ^2E_g state on the nephelauxetic parameter β_1 for oxide compounds. The solid line represents the least-squares fit of the data by expression (6)

As it was mentioned in Introduction, the present study was also motivated by an interest in obtaining luminescent composites of general formula α-Al$_2$O$_3$:Mn^{4+}, Mg^{2+}/GdAG : Ce^{3+}. The one of advantages of such composite materials is the possibility to tune the emission color by changing weight ratio of the components. Yttrium-gadolinium aluminum garnets $(Y_{1-x}Gd_x)_3Al_5O_{12}$ (YGdAG) doped with Ce^{3+} ions are widely used as the effective yellow phosphors for white LEDs. The restricting factors in using such LEDs for general lighting are a low color rendering index ($R_a < 80$) and a high color temperature (> 4000 K) that is caused by a deficit of red component in the emission spectrum of Ce^{3+} doped YGDAG [28; 29]. GdAG : Ce^{3+} is known as a suitable yellow-orange phosphor for warm white LEDs, however, because of the temperature quenching of luminescence, its application is restricted to medium power LEDs [10; 11; 28].

Meanwhile, Al$_2$O$_3$/(Y$_{1-x}$Gd$_x$)$_3$Al$_5$O$_{12}$: Ce^{3+} composite ceramics have been recently proposed as promising materials for high-power LEDs [29]. The positive effect of Al$_2$O$_3$ addition on thermal stability of the ceramics has been attributed to the high thermal conductivity of α-Al$_2$O$_3$ (32–35 W m^{-1}K^{-1}) [29]. In the present work, the use of α-Al$_2$O$_3$: Mn^{4+}, Mg^{2+} as a component of composites had a double purpose: (a) to compensate a deficit of red component in the emission spectrum of Gd$_3$Al$_5$O$_{12}$:Ce^{3+} at the expense of the red emission of Mn^{4+} in α-Al$_2$O$_3$, (b) to improve the thermal stability of composites owing to the high thermal conductivity of α-Al$_2$O$_3$.

As it was mentioned above, the as-prepared α-Al$_2$O$_3$:Mn contains both Mn^{3+} (detected by the diffuse-reflectance spectroscopy) and Mn^{4+} ions, but only Mn^{4+} ions luminesce in α-Al$_2$O$_3$. The same conclusion was made previously for Mn-doped α-Al$_2$O$_3$ obtained by wet chemistry methods [17; 20]. The stabilization of Mn^{4+} in Al$_2$O$_3$ can be provided by the introduction of charge-compensating ions, such as Mg^{2+} into the host lattice [8; 19]. In other words, the introduction of Mg^{2+} should increase the relative concentration of Mn^{4+}. This coincides with the experimental results obtained in the present work. Indeed, from Fig. 6 one can see that the Mg^{2+} co-doping into the α-Al$_2$O$_3$:Mn^{4+} encreases the integrated emission intensity by ∼2.9 times, but it does not result in changes in the Mn^{4+} emission spectrum.

The emission spectra of α-Al$_2$O$_3$:Mn^{4+}, Mg^{2+}/GdAG : Ce^{3+} composites with different weight ratios of the components are compared in Fig. 7. One can see that the spectra are superpositions of a broad band extending from 500 to 800 nm and a narrow one at 678 nm.

It is evident that the broad band with a maximum at 585 nm is caused by the 5d→4f transitions of Ce^{3+} ions in GdAG [10; 11], whereas the band at 678 nm is caused by the Mn^{4+} ^2E_g→$^4A_{2g}$ transitions in α-Al$_2$O$_3$.
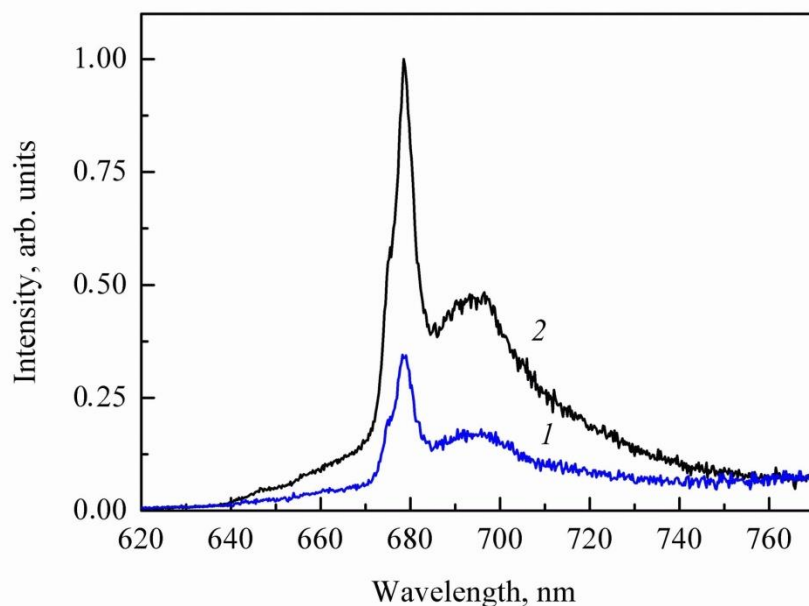
Fig. 6. Effect of the Mg²⁺ co-doping into the Mn- doped α-Al₂O₃. The emission spectra of as-prepared
α-Al₂O₃:Mn³⁺/⁴⁺ (*1*) and α-Al₂O₃:Mn⁴⁺,Mg²⁺ (*2*) were recorded upon excitation at 460 nm
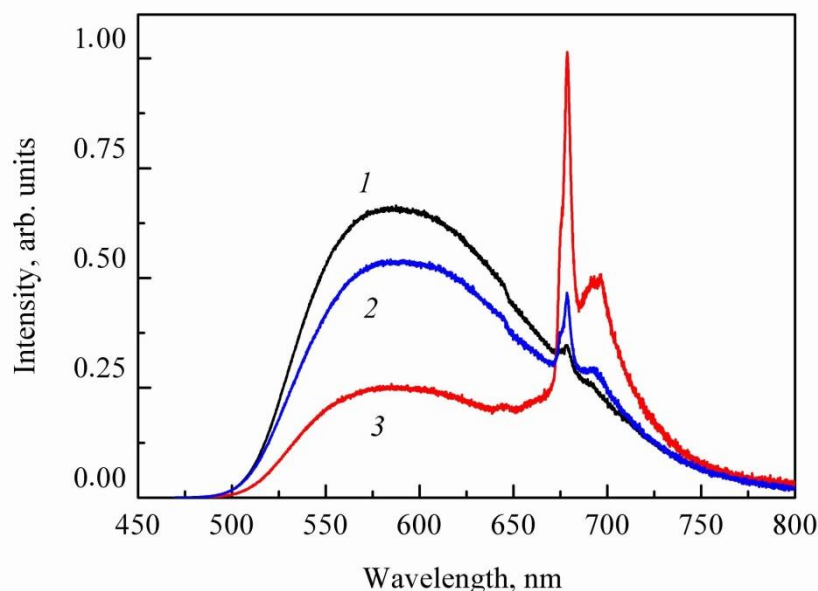
Fig. 7. Comparison of the emission spectra of α-Al₂O₃:Mn⁴⁺,Mg²⁺/GdAG:Ce³⁺ composites with different weight
ratios (N) of the components: N= 1:2 (*1*); 1:1 (*2*); 3:1 (*3*). The spectra were recorded at 293 K upon excitation
with λ_{exc} = 460 nm

It should be noted that the emission color is variable, and it changes from yellow to deep red with increasing content of α-Al₂O₃:Mn⁴⁺, Mg²⁺. The luminescence quantum efficiencies (QE) of the composites were determined as it was described in Ref. [30] using a commercial Y₃Al₅O₁₂:Ce³⁺ phosphor for LEDs with QE = 0.90 as a standard. For the excitation at 460 nm, depending on the weight ratio of the components the QE value was found to vary in the range from 0.52 to ~0.60. These values are comparable with that (QE = 0.58 ± 0.04) of the Ce³⁺ emission in GdAG : Ce³⁺ [11], but they are larger than that (QE = 0.46) reported for Mn⁴⁺ ions in α-Al₂O₃ : Mn⁴⁺, Mg²⁺

ceramic phosphors [8]. The luminescence efficiency of the composites can be enhanced by optimization of the synthesis procedure, Mn⁴⁺-concentration in α-Al₂O₃ and composition modification, but even at this stage quite efficient luminescent materials were obtained.

Conclusions

The Mn⁴⁺-doped α-Al₂O₃ was obtained by combustion method. Based on the results of luminescence measurements, the crystal-field strength (*Dq*) and Racah parameters (*B*, *C*) for Mn⁴⁺ ions in α-Al₂O₃ were determined using the ZPL approach. The obtained values of *Dq* (1898 cm⁻¹) and nephelauxetic parameter β_1

(0.95) for Mn^{4+} ions in the α-Al_2O_3 are conformed to those of Mn^{4+} in other oxide compounds and also to those of Cr^{3+} in the host lattice. In particular, the *Dq/B* value of 2.77 indicates a strong crystal field surrounding of the Mn^{4+} ions in the α-Al_2O_3 lattice. The composites of general formula α-Al_2O_3 : Mn^{4+}, Mg^{2+}/$Gd_3Al_5O_{12}$: Ce^{3+} were also prepared. These materials are shown to exhibit the intense broadband emission with maxima at about 585 and 678 nm. The emission color is variable and it changes from yellow to deep red with increasing content of α-Al_2O_3 : Mn^{4+}, Mg^{2+}. Moreover, the luminescence quantum efficiency of the composites was found as high as 0.60. One can expect that the luminescence efficiency of the composites can be enhanced by optimization of the synthesis conditions and Mn^{4+}-concentration in α-Al_2O_3.

References

[1] Zhou, Q., Dolgov, L., Srivastava, A., M., Zhou, L., Wang, Z., Shi, J., Dramićanin, M. D., Brik, M. G., Wu, M. (2018). Mn^{2+} and Mn^{4+} red phosphors: synthesis, luminescence and applications in WLEDs. A review. *J. Mater. Chem. C, 6*(11), 2652–2671. https://doi.org/10.1039/C8TC00251G.

[2] Adachi, S. (2018). Photoluminescence properties of Mn^{4+}-activated oxide phosphors for use in white-LED applications: A review. *J. Lumin., 202*, 263–281. https://doi.org/10.1016/j.jlumin.2018.05.053.

[3] Li, X., Chen, Z., Wang, B., Liang, R., Li, Y., Kang, L., Liu, P. (2019). Effects of impurity doping on the luminescence performance of Mn^{4+}-doped aluminates with the magnetoplumbite-type structure for plant cultivation. *Materials, 12*, 86. https://doi.org/10.3390/ma12010086.

[4] Sijbom, H. F., Verstraete, R., Joos, J. J., Poelman D., Smet, P. F. (2017). K_2SiF_6:Mn^{4+} as a red phosphor for displays and warm-white LEDs: a review of properties and perspectives. *Opt. Mater. Express, 7*(9), 3332–3365. https://doi.org/10.1364/OME.7.003332.

[5] Brik, M. G., Camardello, S. J., Srivastava, A. M. (2015). Influence of covalency on the Mn^{4+} $^2E_g \rightarrow {}^4A_{2g}$ emission energy in crystals. *ECS J. Solid State Sci. Technol., 4(*3), R39–R43. https://doi.org/10.1149/2.0031503jss.

[6] Brik, M. G., Camardello, S. J., Srivastava, A. M., Avram, N. M., Suchocki, A. (2016). Spin-forbidden transitions in the spectra of transition metal ions and nephelauxetic effect. *ECS J. Solid State Sci. Technol., 5*(1), R3067–R3077. https://doi.org/10.1149/2.0091601jss.

[7] Adachi, S. (2020). Mn^{4+} and Cr^{3+} ions in red and deep red-emitting phosphors: spectral analysis and Racah parameter determination. *J. Lumin., 223*, 117217/1–8. https://doi.org/10.1016/j.jlumin.2020.117217.

[8] Tian, C., Lin, H., Zhang, D., Zhang, P., Hong, R., Han, Z., Qian, X., Zou, J. (2019). Mn^{4+} activated Al_2O_3 red-emitting ceramic phosphor with excellent thermal conductivity. *Opt. Express, 27*(22), 32666–32678. https://doi.org/10.1364/OE.27.032666.

[9] Mykhaylyk, V. B., Kraus, H., Bulyk, L.-I., Lutsyuk, I., Hreb, V., Vasylechko, L., Zhydachevskyy, Y., Wagnera, A., Suchocki, A. (2021). Al_2O_3 co-doped with Cr^{3+} and Mn^{4+}, a dual emitter probe for multimodal non-contact luminescence thermometry. *Dalton Trans., 50*, 4820–14831. https://doi.org/10.1039/D1DT02836G.

[10] Dotsenko, V. P., Berezovskaya, I. V., Voloshinovskii, A. S., Zadneprovskii, B. I., Efryushina, N. P. Luminescence properties and electronic structure of Ce^{3+}-doped gadolinium aluminum garnet. (2015). *Mater. Res. Bull., 64,* 151–155. https://doi.org/10.1016/j.materresbull.2014.12.056.

[11] Berezovskaya, I. V., Voloshinovskii, A. S., Khapko, Z. A., Khomenko, O. V., Efryushina, N. P., Dotsenko, V. P. (2021). Temperature quenching of the Ce^{3+} emission in gadolinium aluminum garnet $Gd_3Al_5O_{12}$. *Func. Mater., 28*(1), 6–13. https://doi.org/10.15407/fm28.01.6.

[12] Jain, A., Koyani, R., Muñoz, C., Sengar, P., Conteras, O. E., Juárez, P., Hirata G. A. (2018). Magnetic-luminescent cerium-doped gadolinium aluminum garnet nanoparticles for simultaneous imaging and photodynamic therapy of cancer cells. *J. Colloid Interface Sci., 526*, 220–229. https://doi.org/10.1016/j.jcis.2018.04.100.

[13] Zolotko, A. N., Poletaev, N. I., Vovchuk, Ya. I. (2015). Gas-disperse synthesis of metal oxide particles. *Comb. Expl. Shock Waves, 51*(2), 252–268. https://doi.org/10.1134/S0010508215020094.

[14] Dotsenko, V. P., Berezovskaya, I. V., Zubar, E. V., Efryushina, N. P., Poletaev, N. I., Doroshenko, Yu. A., Stryganyuk, G. B., Voloshinovskii, A. S. (2013). Synthesis and luminescent study of Ce^{3+}-doped terbium-yttrium aluminum garnet. *J. Alloys Compd., 550,* 159–163. https://doi.org/10.1016/j.jallcom.2012.09.053.

[15] Berezovskaya, I. V., Poletaev, N. I., Khlebnikova, M. E., Zatovsky, I. V., Bychkov, K. L., Efryushina, N. P., Khomenko, E. V., Dotsenko, V. P. (2016). Luminescence study of nanosized Al_2O_3:Tb^{3+} obtained by gas-dispersed synthesis. *Methods Appl. Fluoresce., 4,* 034011/1–8. https://doi.org/10.1088/2050-6120/4/3/034011

[16] Berezovskaya, I. V., Khomenko, E. V., Poletaev, N. I., Khlebnikova, M. E., Stoyanova, I. V., Efryushina, N. P., Dotsenko, V. P. (2018). Oxidation states and microstructure of manganese impurity centers in nanosized Al_2O_3 obtained by combustion method. *Func. Mater., 25*, 490–495. https://doi.org/10.15407/fm25.03.490.

[17] Feofilov, S. P., Kulinkin, A. B., Kutsenko, A. B., Zakharchenya, R. I. (1998). Selective laser spectroscopy of RE^{3+} and Mn^{4+} in sol-gel technique produced Al_2O_3. *J. Lumin., 76 & 77,* 217–220. https://doi.org/10.1016/S0022-2313(97)00204-4.

[18] Baronskiy, M., Rastorguev, A., Zhuzhgov, A., Kostyukov, A., Krivoruchko, O., Snytnikov, V. (2016). Photoluminescence and Raman spectroscopy studies of low-temperature γ-Al_2O_3 phases synthesized from different precursors. *Opt. Mater., 53,* 87–93. https://doi.org/10.1016/j.optmat.2016.01.029.

[19] Geschwind, S., Kisliuk, P., Klein, M. P., Remeika, J. P., Wood D. L. (1962). Sharp-line fluorescence, electron paramagnetic resonance, and thermoluminescence of Mn^{4+} in α-Al_2O_3. *Phys. Rev., 126*(5), 1684–1686. https://doi.org/10.1103/PhysRev.126.1684.

[20] Van Die, A., van der Weg, W. F., Leenaers, A. C. H. I., Blasse, G. (1987). A search for luminescence of the trivalent manganese ion in solid aluminates. *Mat. Res. Bull., 22*, 781–788. https://doi.org/10.1016/0025-5408(87)90032-8.

[21] Kück, S., Hartung, S., Hurling, S., Petermann, K., Huber, G. (1998). Optical transitions in Mn^{3+}-doped garnets. *Phys. Rev. B, 57*(4), 2203–2216. https://doi.org/10.1103/PhysRevB.57.2203.

[22] Noginov, M. A., Loutts, G. B., Warren M. (1999). Spectroscopic studies of Mn^{3+} and Mn^{2+} ions in $YAlO_3$. *J. Opt. Soc. Am. B, 16(*3), 475–483. https://doi.org/10.1364/JOSAB.16.000475.

[23] Srivastava, A. M., Brik, M. G. (2017). The nature of Mn^{4+} luminescence in the orthorhombic perovskite, $GdAlO_3$. *Opt. Mater., 63,* 207–212. https://doi.org/10.1016/j.optmat.2016.06.032.

[24] Adachi, S. (2020). Crystal-field and Racah parameters of Mn^{4+} ion in red and deep red-emitting phosphors: Fluoride versus oxide phosphor. *J. Lumin.*, *218,* 116829/1–8. https://doi.org/10.1016/j.jlumin.2019.116829.

[25] Dotsenko, V. P., Berezovskaya, I. V., Poletaev N. I., Khlebnikova M. E., Zatovsky I. V., Bychkov K. L., Khomenko, E. V., Efryushina, N. P. (2021). Combustion synthesis and nontrivial luminescence properties of nanosized δ^*-Al_2O_3 doped with Cr^{3+} ions. *Solid State Sci., 119,* 106704/1–8.

[26] Adachi, S. (2021). Luminescence spectroscopy of Cr^{3+} in Al_2O_3 polymorphs. *Opt. Mater., 114,* 111000/1–8. https://doi.org/10.1016/j.optmat.2021.111000.

[27] Li, K., Xue, D. (2006). Estimation of electronegativity values of elements in different valence states. *J. Phys. Chem. A, 110*, 11332–11337. https://doi.org/10.1021/jp062886k.

[28] Xia Z., Meijerink A. (2017). Ce^{3+}-Doped garnet phosphors: composition modification, luminescence properties and applications. *Chem. Soc. Rev., 46*, 275–299. https://doi.org/10.1039/C6CS00551A

[29] Li X., Chen J., Liu Z., Deng Z., Huang Q., Huang J., Guo W. (2022). (Ce, Gd):YAG-Al_2O_3 composite ceramics for high-brightness yellow light-emitting diode applications. *J. Eur. Ceram. Soc., 42*, 1121–1131. https://doi.org/10.1016/j.jeurceramsoc.2021.11.027

[30] Katelnikovas, A., Bettentrup, H., Uhlich, D., Sakirzanovas, S., Justel, T., Kareiva, A. (2009). Synthesis and optical properties of Ce^{3+}-doped $Y_3Mg_2AlSi_2O_{12}$. *J. Lumin., 129*, 1356–1361. https://doi.org/10.1016/j.jlumin.2009.07.006